Int. J. Heat Mass Transfer. Vol. 17, pp. 93–107. Pergamon Press 1974. Printed in Great Britain

AN EXPERIMENTAL STUDY OF THE TRANSITION OF NATURAL CONVECTION FLOW ADJACENT TO A VERTICAL SURFACE

FRANCIS GODAUX
SEMA–METRA International, Lisbon, Portugal

and

BENJAMIN GEBHART
Sibley School of Mechanical and Aerospace Engineering, Upson Hall, Cornell University, Ithaca, N.Y. 14850, U.S.A.

(*Received* 5 *May* 1973 *and in revised form* 22 *June* 1973)

Abstract—Events in transition were measured in water, in terms of mean and fluctuating temperature, thermal region thickness and a thermal transition factor. Anemometer measurements were also made. A distinct "thermal" transition mechanism was found. It began downstream of the first signs of velocity field transition. In this delayed region the mean temperature and disturbance quantities gradually assume their turbulent form. In addition, our data indicate that transition events are not accurately predictable solely in terms of the local Grashof number. These first results indicate that the local amount of convected thermal energy is a much better correlator of the transition region location, as well as of other less salient features of transition. A re-examination of previously published data on transition supports this finding.

NOMENCLATURE

c_p, specific heat at constant pressure [J/kg°C];
f, disturbance frequency [Hz];
g, gravitational constant [m/s^2];
G, Grashof parameter for a uniform temperature plate,

$$G = 4\left(\frac{Gr_x}{4}\right)^{\frac{1}{4}};$$

G^*, Grashof parameter for the uniform surface flux plate,

$$G^* = 5\left(\frac{Gr_x^*}{5}\right)^{\frac{1}{4}};$$

Gr_x, local Grashof number based on average plate temperature,

$$Gr_x = \frac{g\beta^* x^3 \Delta T}{\nu^2};$$

Gr_x^*, local Grashof number for a uniform surface flux plate,

$$Gr_x^* = \frac{g\beta^* x^4 q''}{k\nu^2};$$

k, thermal conductivity [J/s m °C];
Pr, Prandtl number,

$$Pr = \frac{c_p}{k}\mu;$$

q'', heat flux at one side of the foil [W/m^2];
s, disturbance temperature amplitude;
T, base flow temperature excess;
T_0, ambient temperature;
T_w, wall temperature;
ΔT, total temperature difference across the boundary layer;
u, velocity in the x direction;
v, velocity in the y direction;
w, velocity in the z direction;
x, coordinate parallel to the plate length;
y, coordinate perpendicular to the plate;
z, coordinate transverse to the plate;

Greek symbols

α, dimensionless wave number,

$$\alpha = \frac{2\pi\delta}{\lambda};$$

β^*, coefficient of volumetric expansion [°C^{-1}];
β, generalized frequency,

$$\beta = \frac{2\pi f\delta}{U};$$

δ, $\delta = 5x/G^*$;
δ_u, velocity boundary layer thickness;
δ_{TM}, measured thermal boundary layer thickness;
δ_{TL}, laminar theoretical thermal boundary layer thickness;
λ, disturbance wave length;
η, dimensionless similarity variable,
$\eta = yG^*/5x$;

μ, viscosity [kg/s m];
ν, kinematic viscosity [m^2/s];
ρ, density [kg/m^3];
Φ, dimensionless temperature, $\phi = (T - T_0)/(T_w - T_0)$;
Γ, thermal transition factor [%].

INTRODUCTION

THIS study is concerned with the processes whereby a natural convection boundary layer eventually undergoes transition from laminar to turbulent conditions, while subject to naturally occurring disturbances. The particular flow is that arising in an extensive ambient water medium, adjacent to a vertical flat surface which dissipates a uniform surface heat flux.

Transition mechanisms have received less attention than laminar aspects of natural convection flow, even though the transition and turbulent regimes are often of more practical importance. In natural convection, as in forced, transport characteristics depend to a large degree on the flow regime. As turbulent flows are frequent in nature and in technology, it is also of prime importance to understand when and how a laminar flow becomes turbulent.

The understanding of such transitions is also a fundamental kind of problem in fluid mechanics. Beginning with the early experiments of Hagen in 1839 and Reynolds in 1883, scientists and engineers have intensely studied these problems in forced flow. Analogous problems in natural convection are now receiving increasing attention because of growing interest in these flows.

The first question concerns the initial cause of instability. This has now been extensively investigated for both types of flows, in both experimental and theoretical studies. A laminar boundary layer first becomes unstable to ever-present disturbances at some distance downstream. Stability theory confirms this. These disturbances eventually lead downstream to laminar breakdown and the production of completely turbulent flow.

The sequence of these latter events is the second important question. Theories and models of these mechanisms are summarized by Stuart [1] for the Blasius flow. It is now expected that, in broad outline, similar processes occur in natural convection flows. It has been shown, conclusively we think, that the initiation of the whole process and the amplification of two dimensional disturbances are likely similar for both flows.

Linear stability theory has been extensively used to study initial instability, disturbance form and amplification characteristics for a variety of natural convection flows and conditions. A wide range of the Prandtl number has also been considered. Many experiments have corroborated many aspects of the predictions, to a remarkable degree and extent. These collected results have even provided an approximate quantitative guide to the eventual beginning and nature of transition. Reference is made to Gebhart [2] and [3] for summaries of these matters.

Audunson and Gebhart [4] have now analyzed nonlinear amplification mechanisms for this flow configuration in air. The treatment is similar to that of Benny and Lin [5] in forced flow. Two dimensional and transverse disturbances were interacted. Nonlinear effects were shown to generate a secondary three dimensional mean motion, Reynolds stresses produced a redistribution of momentum in a plane perpendicular to the direction of the base flow. This secondary mean motion amounts to longitudinal vortices in the boundary region, and even beyond it. They modify the rate of energy transport from the mean flow to disturbances. Thus, in the later stages toward transition, nonlinear interactions have also been shown to become predominant in natural convection flows.

However, a straight-forward analogy to forced flow is now known to be misleading. The last stages of disturbance growth, and of transition, are apparently very different in the weak and buoyancy-coupled flows of natural convection. Although three dimensional effects appear to be very important, the detailed nature of the very last stages of disturbance growth and of transition are still unknown.

The purpose of this study was experimental determination of events in this region. We decided to measure the characteristics of the flow, unguided by any initial presumptions, and to arrive at conclusions guided only by the results.

In our first exploratory hot wire measurements we found that, after a region of three dimensional mean motion, there is a transition region wherein turbulent disturbances first appear in the thicker velocity layer. These apparently cause the first signs of turbulence inside the temperature boundary region. These disturbances do not at first appreciably change the mean temperature profile from the laminar form. However, at higher local Grashof numbers, e.g. further downstream, the velocity disturbances become strong enough to mix with the thinner thermal layer and to begin to diffuse the thermal layer material into the outer velocity layer. At this point the mean temperature profile begins to change form and to overlap much of the velocity layer. We here call this process of turbulent thermal diffusion "thermal" transition.

At the onset of thermal transition we have found that

the thermal boundary layer thickens, the amplitude of the temperature disturbances rapidly increases and the temporal mean temperature distribution begins to deviate significantly from the form of laminar flow. The thermal transition region ends with the development of a completely turbulent boundary region in which all flow variables fluctuate randomly. After this region one expects to find a region of adjustment of the turbulent parameters of scale and intensity, and of the distributions, to the final form of turbulent flow.

Our new understanding of this sequence of events will be detailed later in this study, with the new experimental evidence which supports it. An overall picture of transition, as we now believe it occurs, is given in Fig. 1.

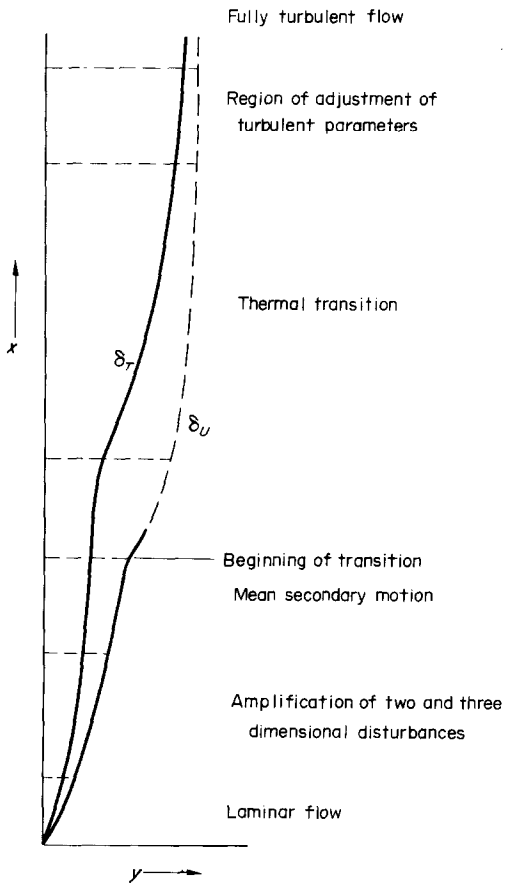

FIG. 1. Mechanism of transition in water.

Few detailed measurements have ever been made in natural convection transition. However, there is some experimental data in the form of both heat transfer correlations and empirical values of the local Grashof number for which transition to turbulence is thought to occur. Mean temperature profiles have also been measured for both the laminar and turbulent regimes and some profiles have incidentally been determined in the region corresponding to what we here call thermal transition. The information which is most directly relevant to our work is given by Warner [6], Cheesewright [7], Lock and deB. Trotter [8] and Vliet and Liu [9]. Tables 1 and 2 summarize all observations known to us concerning values of the local Grashof number characteristic of the beginning of transition and of fully turbulent flow, adjacent to a vertical surface.

These results were obtained with different fluids, heating conditions and surface sizes. The large disagreements suggest that the results in these experiments depended either on local conditions, on the method of observation or on other yet unknown factors. Should local conditions or method successfully explain the tremendous spread of the values for the transition and turbulent Grashof numbers, we would, thereby, reconcile this collection of data with the common opinion, or expectation, that there might exist a small range of value of the local Grashof number, for any given fluid, in which the transition process is expected to occur, independent of the heating rate. Such a criterion for transition is suggested both by tradition and by the studies in linear stability theory which show that the growth rate of two dimensional disturbances depends primarily upon the local Grashof number.

However, it must be remembered that the temperature field drives the motion in natural convection. It is an open question whether any prediction of thermal, transition, or of any transition event, can be based only on the parameters which are important in a linear theory of instability. Strong nonlinear interactions precede turbulence and there may be other important considerations, as we shall see.

As a result, perhaps, of the lack of notable success in attempts to correlate transition with either Gr_x^*, or Ra_x, Vliet and Liu [9] suggested that some other parameter may be required. We known of no attempt to find any dependence of the Grashof number for various transition events on physical quantities like the local heat flux, location of observation x or total local convected energy $Q(x)$.

We also note that a certain amount of confusion inevitably has arisen in studies of transition. No clear definition of transition is apparent for natural convection. This point is particularly important if one accepts the sequence of events we suggest in Fig. 1 for water, a fluid for which the laminar thermal and velocity boundary layer thicknesses are appreciably different.

Table 1. Uniform heat flux condition

Reference	Fluid	Transition G^*	Turbulent G^*	Prandtl number of ambient medium	Geometry of the plate height × width (m × m)
Dotson, reported in Sparrow and Gregg [11]	air	580		0·7	0·71 × 3·05
Colak-Antic [23]	air	600	—	0·7	2·00 × 1·00
Polymeropoulos [25]	nitrogen at high pressure	650–700	—	0·72	0·305 × 0·058
Knowles [26]	silicone	600–700	—	7·7	0·325 × 0·058
Lock and deB. Trotter [8]	water	320–525	550–750	9·8–11·85	0·356 × 0·1525
Vliet and Liu [9]	water	800–1300	1150–2000	10·5–3·6	1·22 × 0·94

In light of these uncertainties, this experimental program was designed to study transition in detail. Qualitative velocity measurements helped us to first formulate the sequence of events shown in Fig. 1. However, we were initially primarily interested in the behaviour of the temperature field. We noticed peculiar characteristics and drastic changes in the field and were led to define what is here called thermal transition. This transition is clearly a sub-event of transition as it is generally understood.

We report in this work several characteristics of the temperature field in the thermal transition region. There are mean temperature profiles, amplitudes of the temperature disturbances, the growth rate of the thermal boundary layer thickness and the predominant frequencies of thermal disturbances. We have also made some measurements of the time distribution of turbulent conditions in the thermal boundary region, in terms of a thermal transition factor later defined.

Thermal transition was studied in a flow adjacent to a vertical surface in water and over a wide range of downstream locations x and of uniform heating rates q''. The events of thermal transition were determined in terms of a local flux Grashof number, actually in terms of G^*.

Our measurements suggest that the thermal transition process is not well correlated by the use of the Grashof number. For all locations and heat flux levels, thermal transition was reasonably well correlated in terms of the quantity $Q(x) = q''x$. This is the total amount of thermal energy given to the boundary layer by the heated surface up to the location x. Particular values of $Q(x)$ are shown to correlate both the beginning and approximate end of thermal transition.

THE EXPERIMENTAL APPARATUS

The experiments were performed in flow adjacent to a 1·3 m high and 0·504 m wide stainless steel foil assembly centered in a large insulated tank of highly purified water. The foil assembly consisted of a sandwich of two layers $1{\cdot}27 \times 10^{-3}$ cm thick inconel

Table 2. Uniform temperature condition

Reference	Fluid	Transition G	Turbulent G	Prandtl number of ambient medium	Geometry of the plate height × width (m × m)
Griffiths and Davis [27]	air	290	660	0·75	
Saunders [28]	air	500	560	0·75	
Saunders [29]	water	400	500	8·0	0·61 × 0·305
Eckert and Soehngen [30]	air	400	—	0·72	0·91 × 0·458
Eckert, Harnett and Irvine [31]	air	830	—	0·7	1·83 × 0·915
Szewcyzk [22]	water	500–850	—	6·7	1·525 × 0·788
Warner [6]	air	650–850	990	0·7	3·72 × 0·61
Cheesewright [7]	air	500–900	900–1040	0·7	2·75 × 0·60
Coutanceau [32]	air	330–500	—	0·7	1·03 × 0·50

600 foil separated by two $1{\cdot}27 \times 10^{-3}$ cm teflon films and two fabric layers of similar thickness. This assembly had been heated under high pressure to fuse the teflon. The resulting combined thickness was $6{\cdot}35 \times 10^{-3}$ cm.

Since the thermal capacity of this assembly was very small, we were able to attain steady flow very quickly, certainly within 2 min. Also, with this large system it was possible to reach turbulent flow with small temperature differences and, thus, with small thermal dissipation. For example, a difference of 10°C, resulted in Gr_x values up to 5×10^{10}, although the usual temperature difference imposed was less than 4°C. This permitted a strictly constant property assumption. As a result of the fast transient and low dissipation, test times up to 25 min were possible without generating appreciable stratification or circulation in the ambient medium. The tank was heavily insulated to isolate it from changes in the environment. The water was vigorously mixed after a test to again equilibrate it.

The foil assembly was stretched between two knife edges to be flat and vertical. This arrangement permitted a complete and well defined boundary layer on both sides of the assembly. In order to provide symmetry at both the leading and trailing edges, the knife edges were in a vertical plane.

The foil was electrically heated by means of a d.c. motor generator set when the required current was more than 30 A, and by an electronic d.c. power supply when the current requirement was less than 30 A. A current of 30 A produced a heat flux level of about 500 W/m^2. The foil current was determined with a digital voltmeter across a calibrated resistance. The voltage across the foil was measured with another digital voltmeter. The input voltage given by the electronic d.c. power supply was very stable. On the other hand, the d.c. generator set was always started 2 h before each run to insure stability of the output voltage.

The foil was located in the center of the tank; the leading edge was 0·145 m from the bottom. The tank was 1·83 m by 0·762 m by 1·83 m high inside and contained about 2300 l. of water. Tank construction materials were teflon and stainless steel. Water treatment facilities are available to achieve a very high water purity and a resistivity level, to $5 \times 10^6\ \Omega$ cm. A stainless filter removed particles above one micron, ion-exchangers demineralized the water, bacteria and organics were filtered and a vacuum deaerater was used. Maintaining such a high level of resistivity is the reason the system was made of stainless steel and teflon. There were two glass windows.

For visualization studies, thermocouple measurements and even for qualitative hot wire anemometry, such a high level of water resistivity is not necessary. However, it is required for very accurate velocity and correlation measurements.

A micrometer traverse assembly positioned both the thermocouple and hot wire probes. The plate location was determined by using an ohmmeter, the resistance becoming very low when the nearest probe contacted the foil.

The temperature, both mean values and thermal disturbances, across the boundary layer was determined by means of an array of four Chromel–Constantan thermocouples made of one mil diameter wire. This size gave a response time of the order of 2 ms.

The thermocouple wires were thinly coated with teflon for electrical insulation. This protection was removed at the ends to weld the junction. The wires were held by hollow glass tubes of 1 mm dia of 7 cm length. These probes looked much like hot wire probes. The supporting tubes were parallel to the base flow and were supported by a small stainless steel frame perpendicular to the heated surface. The junction nearest the surface could touch it. The distances of the second, the third and the fourth junctions, from the nearest one, were 5, 10 and 20 mm. The main probe support was entirely outside the boundary layer. By traversing the array, the entire temperature field across the boundary layer could be recorded very quickly.

The four thermocouple circuits were independent of each other. Using a temperature reference of 0°C (ice) the signals were fed into four channels of a Beckmann recorder. A small amplitude noise, of high frequency with respect to the natural frequencies of the phenomena, was filtered out. We were able to use a very high sensitivity range with the recorder (of the order of 10 μV/cm). This permitted the detection of very small temperature disturbances, since the sensitivity on the chart was 0·2°C/cm.

Hot wires were used to get qualitative information on the development of the velocity disturbances in the transition region. The probe, made of platinum wire, was positioned at less than 2 mm from the second thermocouple of the array and in the same plane (xz), parallel to the plate, to permit simultaneous measurement of both velocity and temperature disturbances at essentially the same distance from the surface y. We shall see later that this capability was very important when the second thermocouple was at the edge of the thermal boundary layer. The anemometer (Disa Model 55D01) signal was also recorded. The hot wire was normal to the x and y directions and, therefore, directly measured essentially the longitudinal velocity component u. Being rather more

interested in the occurrence and time development of velocity disturbances, than in their absolute amplitudes, we did not individually calibrate the particular hot wire probe used. In natural convection this is a more sophisticated procedure than in forced flows, as discussed by Hollasch and Gebhart [10].

All the measurements were made late in the evening and during the night, to avoid the effects of many large disturbances arising from building use during the day. After each test, a propeller mixed the tank water to remove stratification and insure uniform thermal conditions for the next test. Several experiments were made at different dates, at the same location in x, to see whether unknown and changing effects had influenced the results. In all such checks, no appreciable differences were noticed between experiments made on different days.

One particular characteristic of our experimental technique must be explained at the outset, to make the nature of our data presentation clear and to avoid later confusion. What we wished to do was to measure flow characteristics over a wide range of $G^* \propto (x^4 q'')^{\frac{1}{5}}$. This quantity is usually thought of as varying downstream, on a given surface and for a given heating condition q'', due to changing x. However, it was not convenient in these experiments to vary G^* entirely by varying x. That would have required frequent transversing of the sensors. This is difficult and would have required many tedious determinations of the exact distance scale, y, normal to the surface. Therefore, measurements were made at a number of selected values of x. A range of G^* was obtained at each location by varying q''. Thus, the events for a range of G^* were actually obtained at each x.

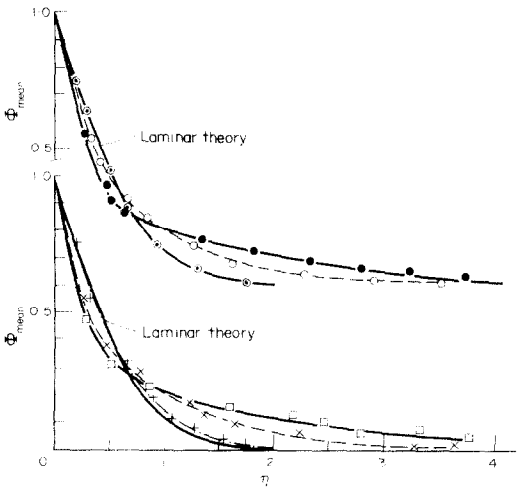

FIG. 2. Mean temperature distributions.

Data:

	x (cm)	G^*	$\Gamma(\eta = 2{\cdot}5)$		x (cm)	G^*	$\Gamma(\eta = 2{\cdot}5)$
✱	36·2	485	0	+	100	948	0·05
○	36·2	608	0·18	×	100	1031	0·6
●	36·2	625	0·68	□	100	1131	0·9

EXPERIMENTAL RESULTS AND OBSERVATIONS

1. *Mean temperature distributions and thermal boundary layer thickness*

We first measured the mean temperature distributions in what was evidently transition flow. Characteristic results, generalized as the normalized temperature $\Phi = T - T_0/T_w - T_0$, are plotted in Fig. 2 in terms of the laminar similarity variable $\eta = y/\delta = yG^*/5x$. Data is shown for two locations, $x = 36{\cdot}2$ cm and $x = 100$ cm. In addition to the experimental points and the curves which fit them, we also show the curve calculated by Sparrow and Gregg [11] for steady laminar flow.

We did not measure the temperature profile near the wall to the detail obtained by Warner [6] and by Cheesewright [7], being rather interested in the development of the outer part of the profiles. The temperature of the surface itself was estimated by pushing the closest junction of the thermocouple array against it.

These mean temperature distributions show the change in the form of the thermal boundary layer from laminar conditions and during transition toward completely turbulent flow. The profile measured at $x = 36{\cdot}2$ cm for $G^* = 485$ is in good agreement with the laminar theory as are the results at $x = 100$ cm for $G^* = 948$, even though the thermal layer thickness appears already to be increasing. However, the temperature profiles for $G^* = 625$ at $x = 36{\cdot}2$ cm and $G^* = 1130$ at $x = 100$ cm are much thickened and changed, presumably by turbulent transport. Intermediate values of G^* appear to give intermediate profiles in what is herein called the thermal transition process.

The thermal transition factor Γ for each flow condition is listed in the figure captions. This factor was determined from the instantaneous local temperature records and is defined as the fraction of the observation time during which turbulent temperature fluctuations occur. Its numerical value should correlate thermal transition and the development of turbulence.

Increasing values of Γ clearly do go with the changes in the mean temperature profile. We found $\Gamma \approx 0$ for the profiles at lower G^*, which were essentially in agreement with the laminar theory. At higher G^* the increased steepening at low η and flattening at higher η are accompanied by increasing Γ. We note, incidentally, that with the development of thermal

transition, further profile changes occur mostly in the outer region and amount to a large increase in thermal boundary layer thickness.

The measured thermal boundary layer thickness, δ_{TM}, scaled with the theoretical laminar thickness $\delta_{TL} = 2{\cdot}06\,\delta$, is plotted in Fig. 3 in terms of x, q'' and G^*. Thermal boundary layer thickness δ_{TM} is defined, as usual, as the distance out from the surface at which the mean temperature difference is only 1 per cent of the overall temperature difference. Given the very flat mean temperature profile, these estimations of δ_{TM} do not have very high accuracy. To construct Fig. 3, data points at the same x and q'' were connected by curves.

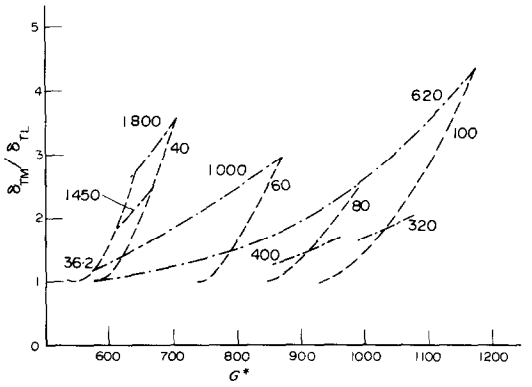

FIG. 3. Thermal boundary layer thickness variation in thermal transition.
Data: ———, constant x (x in cm)
·—·—·, constant q'' (q'' in W/m²)

The first data at each x were, apparently, laminar flow. We see that transition begins at lower G^* and proceeds more rapidly for higher flux levels, This implies one of the most important of our findings, as will be discussed later in detail. Incidentally, the progression of a particular thermal transition is seen by a constant q'' curve. The only extensive one shown is for $q'' = 620$ W/m².

Figure 2 clearly shows that the laminar similarity variable $\eta(= y/\delta)$ does not correlate the mean temperature profiles during thermal transition. Figure 4 shows that y/δ_{TM} does no better. A systematic disagreement remains which cannot be removed while using y in the abscissa. Thus, attempts made in several studies to correlate turbulent data by scaling y cannot correlate thermal transition. If any correlation exists, a normalization must be related both to the thickness of the thermal boundary layer and to some additional y dependent quantity, e.g. the local thermal transition factor Γ.

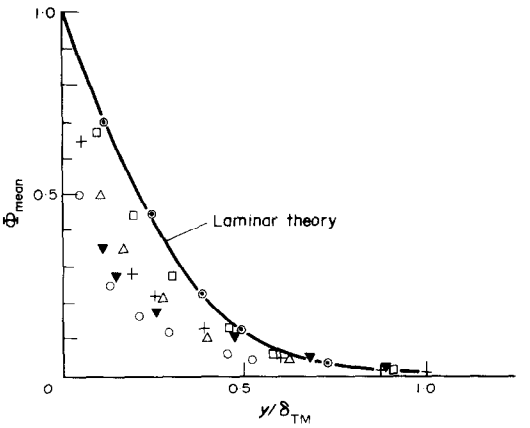

FIG. 4. Mean temperature distributions

Data:

x(cm)	G^*	$\Gamma(\eta=2{\cdot}5)$	x(cm)	G^*	$\Gamma(\eta=2{\cdot}5)$
⊛ 36·2	485	0·0	□ 100	948	0·05
△ 36·2	608	0·18	+ 100	1031	0·6
▼ 36·2	625	0·68	○ 100	1130	0·9

2. Temperature disturbances across the boundary layer

The foregoing results indicate that, with thermal transition, the mean temperature profiles develop larger gradients near the surface and extend further out. We have also found that this increase of the thermal boundary layer thickness is accompanied by an increase in the amplitudes of the temperature disturbances. The measured disturbance amplitude distributions across the boundary region are plotted in Fig. 5, for $x = 36{\cdot}2$ and 100 cm and for several values of the surface heat flux q''. These values have been normalized with the largest value measured s_m. Corresponding values of G^* and Γ are given.

A theoretical distribution of temperature disturbance amplitude is also plotted as computed by Dring and Gebhart [12] from linear stability theory for two dimensional disturbances at $G^* = 300$ and for the β which corresponded to 0·11 Hz for their experimental conditions. The peak value of s is seen to occur at around $\eta = 0{\cdot}9$.

During transition, the disturbance amplitude distribution is shifted increasingly toward the surface. For both x locations, and for the lowest G^* and Γ, our experimental data are in accord with the theoretical laminar curve. The measurements of Dring and Gebhart [13], with controlled disturbances, had also corroborated this calculation.

The present disturbance amplitude data apparently do not appear to go to a zero value at the surface. This suggests that the disturbance coupling predicted by Knowles and Gebhart [14] in laminar flow, for surfaces of relatively small thermal capacity, also occurs during thermal transition.

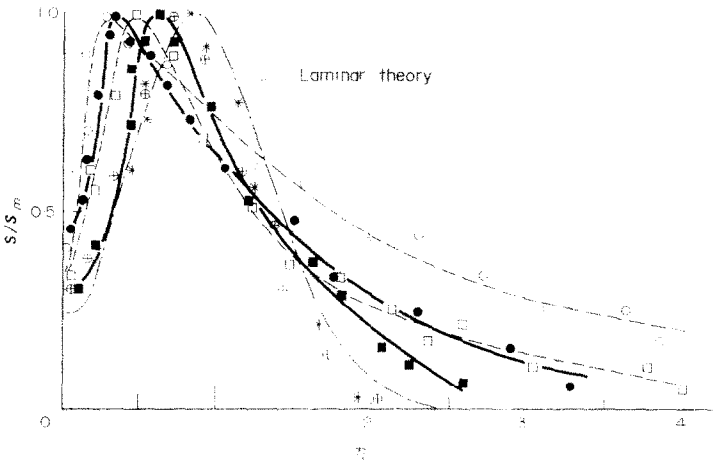

FIG. 5. The disturbance temperature profiles.

Data:

x (cm)	G^*	$\Gamma(\eta=2{\cdot}5)$	x (cm)	G^*	$\Gamma(\eta=2{\cdot}5)$
★ 36·2	574	0·05	✧ 36·2	948	0·05
■ 36·2	608	0·18	□ 100	1031	0·6
● 36·2	640	0·95	○ 100	1176	1·0

Theory: $G^* = 300$, $f = 0{\cdot}11$ Hz.

For higher Grashof numbers, the region of appreciable fluctuations extends out to higher η. This is related to the growth of the thermal boundary layer thickness.

In Fig. 6, the highest measured amplitude of the temperature disturbances in the boundary region is plotted vs location in x and for several values of heat flux. The data were scaled by the total measured temperature difference across the boundary layer. These results show that the occurrence of thermal transition, which we saw causes a drastic change in the mean temperature profiles, is also characterized by a sudden increase in the magnitude of the disturbances. For high Grashof numbers, further into the thermal transition region, the rate of increase slackens. As we approach fully turbulent conditions, the highest amplitudes of the temperature disturbances increase to the order of 60 per cent of the total temperature difference across the boundary layer. This leads us to conclude, with Lock and deB. Trotter, that the scale of turbulence is significantly larger in natural convection than found in comparable forced convection flows.

3. *Predominant frequencies of the natural temperature disturbances*

In Fig. 7, we have plotted, for different locations and values of the surface heat flux, the measured predominant frequencies of the natural temperature disturbances in the thermal transition region. The results are given both in terms of f and β. They were obtained from the same experimental chart records used to

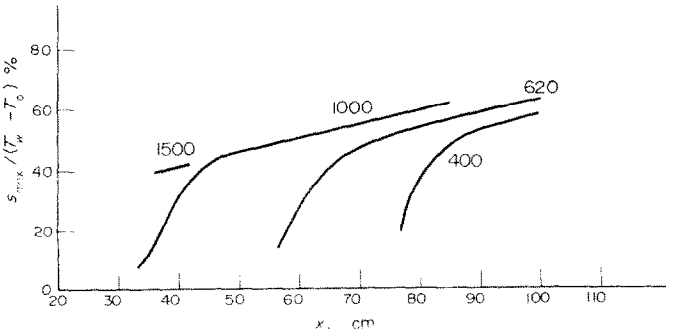

FIG. 6. Distributions of highest amplitude temperature disturbances, for different heat fluxes q'' in W/m^2.

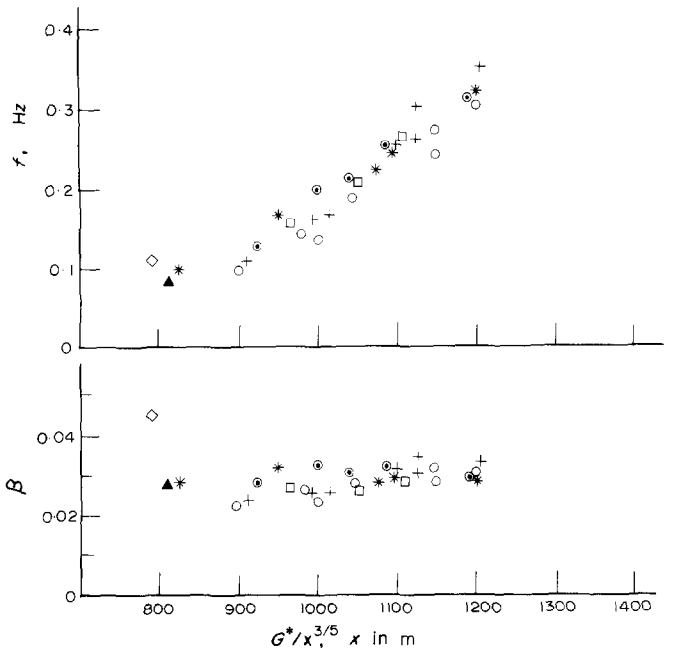

FIG. 7. Predominant frequencies of natural temperature disturbances.

Data:
- ◉ $x = 36{\cdot}2$ cm
- □ $x = 40$ cm
- ★ $x = 60$ cm
- \+ $x = 80$ cm
- ○ $x = 100$ cm
- ◇ Dring and Gebhart [13]
- ▲ Jaluria [16] for $x = 60$ cm

measure the amplitudes and were determined at locations in the boundary layer such that η was less than two, i.e. within the thickness of a laminar thermal layer. The range of frequency found is seen to be from 0·08 to 0·35 Hz.

The frequencies are seen to increase with the Grasof number. However, the abscissa $G^*/x^{\frac{3}{2}}$ was found to collect points from all locations into a more-or-less single definite trend. When the frequency f is generalized as $\beta = 2\pi f\delta/U$, as in linear stability theory, our new data are all seen to be between 0·02 and 0·035. Thus, δ/U, calculated as though the flow was locally laminar, has greatly reduced the frequency variation with $G^*/x^{\frac{3}{2}}$.

The most important aspect of this result is that all of these β, G^* points are close to the constant frequency trajectory of maximum disturbance amplification calculated from stability theory by Hieber and Gebhart [15]. These data points are also plotted on this stability plane in Fig. 8. We see that the filtering effect predicted by the stability theory is again found and again well beyond the range of linear processes, as pointed out by Gebhart [2] from other data.

The fact that the predominant naturally arising frequency depends upon $G^*/x^{\frac{3}{2}}$ suggests that such a parameter has a very important role in characterizing the transition process. This quantity will later arise in another consideration.

In Fig. 7, our data points for $G^*/x^{\frac{3}{2}}$ equal to 825 and to 900 ($m^{-\frac{3}{2}}$) have interesting implications. They are seen to span the range from highly filtered two dimensional disturbances to the trend of the three dimensional disturbances which prevails at higher $G^*/x^{\frac{3}{2}}$ during thermal transition. These two determinations were made both by looking at the recordings of temperature and at a Schlieren visualization of the thermal boundary layer. For the frequency at 825, simple two dimensional disturbances were found when the recording of temperature still showed regular sinusoidal fluctuations. The disturbances were no longer regular and simple-periodic at 900, appreciable other components had appeared.

The point shown from Jaluria [16] was obtained in another experimental set-up. It was measured for a highly amplified three dimensional disturbance in a controlled experiment. The point from Dring and Gebhart [13] corresponds to two dimensional disturbances. All the other points are in the thermal transition region. Thus, we may approximately locate the lower and perhaps also the upper boundaries of the various thermal transition processes from the range seen in Fig. 7.

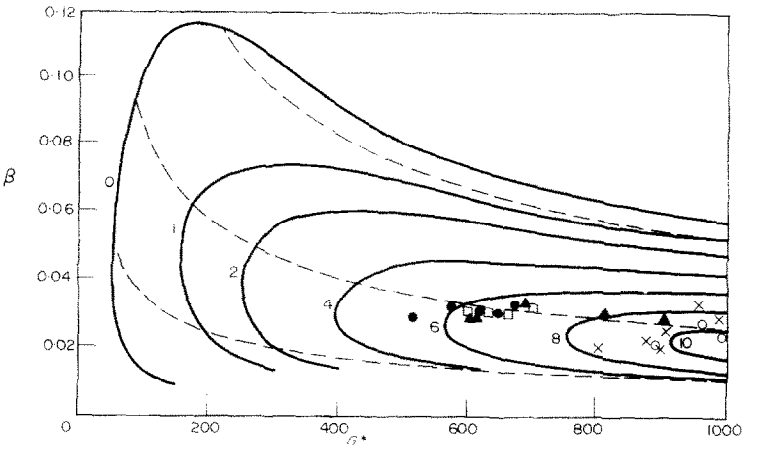

FIG. 8. Stability plane for $Pr = 6{\cdot}7$ (Hieber and Gebhart [15]) showing amplitude ratio contours in the unstable region. The data points are in the thermal transition region.
Data: ●, $x = 36{\cdot}2$ cm; □, $x = 40$ cm; ▲, $x = 60$ cm; ×, $x = 80$ cm; ○, $x = 100$ cm.

The variation of the predominant physical frequency during thermal transition, with Grashof number, means that, for a constant surface heat flux, the frequency begins to vary downstream during thermal transition. Our data on Fig. 8 suggest the same thing. This does not occur in the laminar region of the boundary layer, where the physical frequency of a disturbance is being essentially conserved downstream. Thus, thermal transition appears to result in higher principal frequencies than those corresponding to two and three dimensional disturbances in still laminar flow.

The mechanism of this transformation of the physical frequency is still unknown. The experimental frequency (0·11 Hz at $G^* = 300$) from Dring and Gebhart, in laminar conditions and for controlled two dimensional disturbances, is also outside the trend found in thermal transition.

One possible explanation of this frequency increase may be as follows. The natural disturbances entering the boundary layer and later amplified are presumably random, and therefore, are characterized by a number of different frequencies. Although stability theory does predict a sharp downstream filtering effect, the band of favored frequencies is still wide enough to amplify disturbances over some frequency range.

Another consideration is that these higher measured frequencies correspond to deeper stages of thermal transition and are known with less accuracy. The measured disturbances are no longer simply sinusoidal, making the determination of the principal period of fluctuation more difficult and less accurate. One might consider determining the principal frequency by filtering or through a spectral analysis. However, this is a very difficult instrumentation problem at this frequency level.

We conclude from these results that the principal frequency in thermal transition varies approximately linearly with the parameter $G^*/x^{\frac{1}{4}}$. Also, at the beginning of thermal transition, the physical frequencies seem to be approximately the same for different levels of the surface heat flux, even at different locations of observation x.

4. *Development of turbulence in the outer part of the region*

The beginning of thermal transition has thus been found to be signalled by deviation of the temporal mean temperature field, increasing growth rate of the thermal boundary layer, large local temperature fluctuations, and an increase in the predominant disturbance frequency. The temperature disturbances penetrate the outer part of the boundary region as turbulent disturbances increasingly, downstream, mix fluid from the vicinity of the surface into the outer part of the velocity boundary layer. Just after the beginning of thermal transition, these eddies are few in number and small in size. Our measurements show that they grow as they are convected downstream.

In order to characterize the growth of thermal turbulence we have calculated the local thermal transition factor Γ, as previously defined. Typical results, seen in Fig. 9, were obtained at three different locations in x and different heat flux levels and, therefore, at different values of G^*.

We see that Γ increases uniformly with G^*. The highest G^* values for which such curves still go quickly

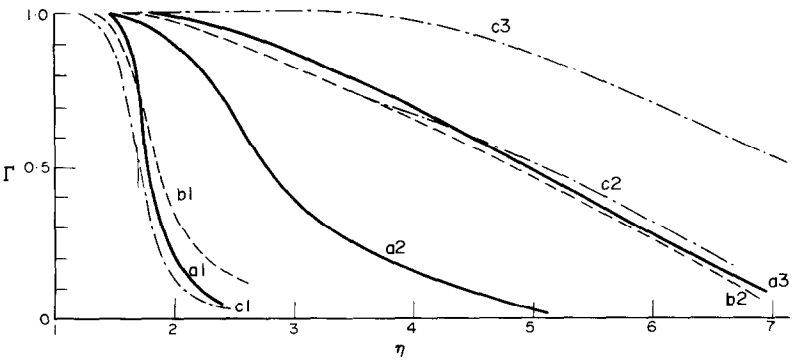

FIG. 9. Variation of the thermal transition factor with x and q''.

Data:	x (cm)	G^*	G^*	G^*
———	36·2	574, a1	625, a2	640, a3
– – – –	60	791, b1	879, b2	
–·–·–·	100	948, c1	1131, c2	1176, c3

to zero near $\eta = 2$, i.e. at the edge of the laminar thermal boundary layer, correspond to the beginning of processes termed here as thermal transition. Values of G^* for which Γ remains near 1·0 through the whole boundary region correspond to conditions approaching complete thermal turbulence. Thus, a measure of the transition region is the distance, in x, between these two conditions.

However, the most striking characteristic of the behavior of Γ is the unexpected behavior at low values of η, i.e. inside the extent of a nominally laminar thermal boundary layer. Values of essentially 1·0 are found there. This means that at the beginning of thermal transition the thermal boundary layer is already highly disturbed although still at the thickness of the original laminar one. We have already seen that this material progressively mixes downstream with the cold fluid outside.

In an attempt to determine the cause of this apparent earlier transition, a hot-wire probe was added to the thermocouple array. The velocity u in the streamwise direction was measured, along with the temperature disturbances. At locations, in x or q'', before the beginning of thermal transition, the hotwire detected the presence of turbulence in the velocity field and outside the extent of the laminar thermal layer. The temperature was essentially T_0, as we have seen. The velocity turbulence level increased with G^*. Sudden decreases of velocity were followed by slower increases. Although these variations resembled spikes, the velocity record did not show a pronounced intermittent pattern similar to that familiar in forced flow transition, either before or after the beginning of thermal transition. There were signs of turbulence but it was not possible to make any quantitative determinations from this data.

The fact that the thickness of the thermal layer is much less than that of the velocity layer is of primary importance in interpreting our measurements. We might perhaps conclude from other considerations, Audunson and Gebhart [4], that the genesis of turbulence arises at shear layers which may form near the velocity inflexion point. This is at the outer edge of the thermal layer. If turbulence initially arises there, the disturbances would at first be of small intensity and not initially strong enough to immediately reach in and diffuse fluid from deep in the thermal layer out into that outside. However, these disturbances are apparently sufficiently vigorous to cause the high values of Γ at $\eta < 2$ seen before the beginning of thermal transition.

The scale and intensity of the velocity disturbances increases with x. They apparently become large enough to disrupt the temperature layer and thus begin the onset of thermal transition. The intensity of the temperature disturbances then increases downstream.

This postulated mechanism is a more complicated one than observed heretofore in the transition of other flows. It is a consequence of velocity–temperature coupling as well as of the effect of the Prandtl number in causing different thermal and velocity layer thicknesses.

For air these two layers are of nearly equal thickness and we would expect thermal transition to occur almost simultaneously with transition in the velocity field. Recall that the thermal boundary layer overlays the inflexion region. If turbulence is born

there it may simultaneously produce thermal transition. Any delay in turbulent diffusion would be a consequence of the concentration of the largest temperature difference near the surface and well inside the region of the largest velocity disturbances.

Our mechanism of transition is postulated from both immediate and posterior consequences. The validity of the postulate must next be tested by direct and detailed study of the transition effect occurring before what is here called thermal transition.

5. *Boundaries of the thermal transition region*

We have seen that the Grashof number does not correlate thermal transition. Relevant values of G^* vary with the level of q''. The variation of G^* with x for the beginning of thermal transition is plotted in Fig. 10. Recall that G^* is a function of x and q''. We see that, in the x range from 36·2 to 100 cm, the values of G^* at the beginning of thermal transition depend, very approximately, on $x^{\frac{1}{2}}$. Thus, thermal transition begins as $G^*/x^{\frac{1}{2}}$ reaches a certain value. This parameter also approximately correlated disturbance frequencies.

The ratio $G^*/x^{\frac{1}{2}}$ has an interesting physical interpretation. Since G^* is proportional to $(q''x^4)^{\frac{1}{5}}$, this ratio is proportional to $(q''x)^{\frac{1}{5}}$ and to $Q(x)^{\frac{1}{5}}$, where $Q(x)$ is the total amount of thermal energy being convected locally in the boundary region at x. The correlations of our data shown in Fig. 10 are plotted in Fig. 11 in terms of $Q(x)$ vs x. Points for the beginning of transition are seen to lie at around 370 W/m. The band for the approximate end of thermal transition is at around 650 W/m.

The several points obtained from each Warner and Cheesewright, also strongly suggest that the thermal transition in air approximately correlates in terms of $Q(x)$. Limiting values of approximately 90 and 180 W/m, respectively, infer that thermal transition in air is also related to the amount of thermal energy carried in the boundary layer. Other data collected in Tables 1 and 2 also suggest in Fig. 10 a dependence of the transition and turbulent Grashof numbers on the experimental conditions. The height of observation is always limited by the height of the surface used and in the absence of a specification of the exact location of observed transition we have used the height of the

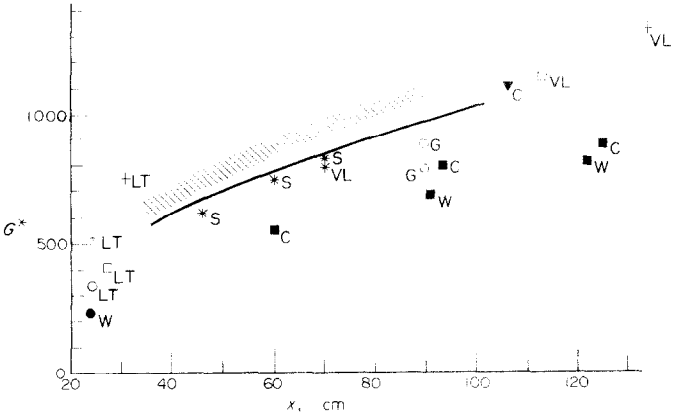

FIG. 10. Events of transition.
From data of the present study: ———, G^* at the beginning of thermal transition.
Other data: laminar conditions, ○, water, ●, air;
beginning of thermal transition, ⋆, water;
thermal transition, □, water, ■, air;
complete turbulence, +, water, ▼, air.
Notation: G, present study; C, Cheesewright; LT, Lock and deB. Trotter;
S, Szewczyk; VL, Vliet and Liu; W, Warner.

The approximate variation of G^* with x for $\Gamma \approx 1{\cdot}0$ is also shown on Fig. 10, as a shaded region because of less reliability of the data. This limit also depends upon x. We recall that the combination $G^*/x^{\frac{1}{2}}$ was used to correlate the predominant frequencies of natural temperature disturbances in the thermal transition region.

surface to reduce the data to our parameters. The data of Lock and deB. Trotter and Vliet and Liu for water, also show such a variation. In spite of the scatter, there is a similar trend of G^* at transition.

There is a parallel to this unexpected result in forced convection flows. Many studies have shown that the Reynolds number by itself is not a unique

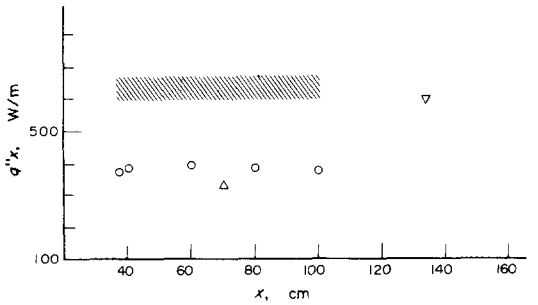

FIG. 11. Values of $Q(x) = q''x$ for transition in water.
Data: ▨, approximate end of thermal transition;
○, beginning of thermal transition;
△, Vliet and Liu, beginning of thermal transition;
▽, Vliet and Liu, beginning of complete turbulence.

criterion for transition and turbulence, for example, that of Tani [17] for boundary layer flows and of Gaviglio and Burnage [18] for water and for flow inside tubes. Coles [19] reviewed experiments on intermittency in pipe, circular Couette, boundary layer and fully developed free shear flow in wakes and jets, and concluded that transition could not be correlated by the Reynolds number alone, either in flows where the Reynolds number was either constant or varied with x. Monin and Yaglom [20], in discussing the problem of transition in forced flows, reach the same conclusions.

The simple presumption that transition to turbulence occurs at unique values of G^* or Re stems from the earliest studies of fluid mechanics and presumption was strengthened by the fact that many linear theories of hydrodynamic stability successfully explain both neutral stability as well as the early amplification of two dimensional disturbances in boundary layers in terms of G^* and Re. However, this is based on many assumptions, such as linearity and parallel flow. Even the inclusion of x direction gradients does not result in Orr–Sommerfeld equations. In addition to the usual parameters G^*, Pr, α and β, the x dependent quantities U and δ are added.

Nonlinear phenomena also intervene. The study of Audunson and Gebhart extend linear theory for a natural convection flow. Nonlinear interactions lead to secondary mean flows which may provide sufficient conditions for transition. However, even these effects, by themselves, are not likely to be the final mechanisms for turbulence production.

MECHANISMS OF TRANSITION

Many aspects of the long and complicated process of transition of an initially stable laminar natural convection boundary layer flow to turbulence are now well understood. In the first stage small disturbances enter the laminar flow from the surrounding medium and become two dimensional. As they are convected downstream, a strong filtering effect amplifies only a narrow band of frequencies and disturbance energy becomes concentrated at essentially a single frequency. These simple oscillations are suggested by Schlieren and interferometric observations. Local sensors indicate nearly perfect sinusoidal form. The second stage is the amplification of transverse disturbances and their interaction with the two dimensional ones. Secondary mean flows arise. At this point uncertainties arise concerning subsequent mechanisms.

Consideration of such mechanisms in forced flow caused much controversy. Until Klebanoff, Tidstrom and Sargent [21] established that secondary mean flow longitudinal vortices occur in conjunction with nonlinear three dimensional interaction, other explanations had been advanced: generation of higher harmonics, the effects of concave streamline curvature associated with the wave motion, the vortex loop formation. It is now generally conceded that these latter effects are not adequate, that they do not dominate the overall behavior of transition. It is the interaction of disturbances with the mean flow, through Reynolds stresses, that apparently produces the secondary mean flow longitudinal vortices which lead to transition.

The same kind of difference of opinion arose concerning transition mechanisms in natural convection flows. Szewczyk [22] saw transverse vorticity components by dye visualization and defended a theory of vortex loop formation. However, the observations of Colak-Antic [23] strongly indicated the existence of longitudinal vortices. The presence of intense, concentrated shear layers was inferred. This mechanism is also supported by the computations of Audunson and Gebhart and by a controlled experiment by Jaluria and Gebhart [24]. As in the Blasius flow, the secondary mean motion is a nonlinear interaction of two dimensional and transverse disturbances. A double longitudinal eddy system results. Mean momentum and thermal energy are redistributed both in the spanwise and normal directions, including alternate spanwise concentrations of high shear layer. This, or other consequences of the vortex system, seem now to be the immediate cause of laminar flow breakdown.

The third stage, breakdown, is apparently different and more complicated than in forced convection where it is thought that the shear layer is instrumental. The shear layer, as a secondary instability, generates rapidly oscillating "spike-like" disturbances. These are produced intermittently in the boundary layer

and immediately precede the formation of turbulent bursts.

On the other hand, we have found in water that the velocity field first showed signs of turbulence. We also did not find intermittent bursts resembling those characteristic of forced flow transition. Only further downstream do the velocity disturbances alter the mean temperature profile. This is the beginning of thermal transition. The thickness of the thermal layer then rapidly increases. The fluctuations of the temperature grow in amplitude and expand outward.

At still higher Grashof numbers the mixing process becomes so intense that it is no longer possible to find any vestige of the laminar flow. It is expected that this condition is followed by a region of further adjustment of the turbulent parameters to what might be called fully developed turbulent flow. Thus, the final breakdown to turbulence is not a sudden spatial phenomenon, but is itself also a sequence of coupled mechanisms.

Therefore, transition in such a flow as this is not to be understood in detail only in terms of a conversion of the velocity field to turbulence. The special significance of both the Prandtl number and of velocity–temperature coupling in natural convection flows dictate much more complicated mechanisms.

CONCLUSIONS

The region of transition in water is divided into two coupled and partially overlapping subregions. In the first, the velocity loses its laminar form on the way to turbulence. The second subregion, here called thermal transition, begins later. The events of transition are not correlated by the local Grashof number. Thermal transition appears to begin when the total amount of convected thermal energy, $Q(x) = q''x$, has reached some particular value. A re-examination of data from other experiments concerning transition, in both air and water, suggests some such similar effect.

Acknowledgements—The writers wish to express their appreciation for the support of the National Science Foundation under Grant GK 18529. This has made possible the equipment, instruments, as well as much of the time necessary for this study.

REFERENCES

1. J. T. Stuart, Hydrodynamic stability, *Appl. Mech. Rev.* **18**, 523 (1965).
2. B. Gebhart, Natural convection flow, instability and transition, *J. Heat Transfer* **91**, 293 (1969).
3. B. Gebhart, Instability, transition and turbulence in buoyancy-induced flows, *Ann. Rev. Fluid Mech.* **5**, 213 (1973).
4. T. Audunson and B. Gebhart, Observations on the secondary mean motion induced by oscillations in a natural convection flow, submitted for publication.
5. D. J. Benney and C. C. Lin, On the secondary motion induced by oscillations in a shear flow, *Physics Fluids* **3**, 656 (1960).
6. C. Warner, Turbulent natural convection in air along a vertical flat plate, Ph.D. Thesis, The University of Michigan (1966). See also: C. Warner and V. S. Arpaci, An experimental investigation of turbulent natural convection in air at low pressure along a vertical heated plate, *Int. J. Heat Mass Transfer* **11**, 397 (1968).
7. R. Cheesewright, Turbulent natural convection from a vertical plane surface, *J. Heat Transfer* **90**, 1 (1968).
8. G. S. H. Lock and F. J. deB. Trotter, Observations on the structure of a turbulent free convection boundary layer, *Int. J. Heat Mass Transfer* **11**, 1225 (1968).
9. G. C. Vliet and C. K. Liu, An experimental study of turbulent natural convection boundary layers, *J. Heat Transfer* **91**, 517 (1969).
10. K. Hollasch and B. Gebhart, Calibration of constant temperature hot-wire anemometers at low velocity in water with variable fluid temperatures, *J. Heat Transfer* **94**, 17–22 (1972).
11. E. M. Sparrow and J. L. Gregg, Laminar free convection from a vertical plate with uniform surface heat flux, *Trans. Am. Soc. Mech. Engrs* **78**, 435 (1956).
12. R. P. Dring and B. Gebhart, A theoretical investigation of disturbance amplification in external laminar natural convection, *J. Fluid Mech.* **34**, 551 (1968).
13. R. P. Dring and B. Gebhart, An experimental investigation of disturbance amplification in external laminar natural convection flow, *J. Fluid Mech.* **36**, 447 (1969).
14. C. P. Knowles and B. Gebhart, The stability of the laminar natural convection boundary layer, *J. Fluid Mech.* **34**, 657 (1968).
15. C. A. Hieber and B. Gebhart, Stability of vertical natural convection boundary layers: some numerical solutions, *J. Fluid Mech.* **48**, 625 (1971).
16. Y. Jaluria, The growth and propagation of three dimensional disturbances in laminar natural convection, M.S. Thesis, Cornell University (1972).
17. I. Tani, Boundary layer transition, *Ann. Rev. Fluid Mech.* **1** (1969).
18. J. Gaviglio and H. Burnage, Sur l'intermittence de transition de l'état laminaire à état turbulent dans divers écoulements, *J. Mécanique* **9** (1) (1970).
19. D. Coles, Interfaces and intermittency in turbulent shear flows, paper in *Mècanique de la Turbulence*. Colloque International du CNRS à Marseille, Ed. du CNRS, Paris (1962).
20. A. S. Monin and A. M. Yaglom, *Statistical Fluid Mechanics: Mechanics of Turbulence*, Volume I. MIT Press, Cambridge (1971).
21. P. S. Klebanoff, K. D. Tidstrom and L. M. Sargent, The three dimensional nature of boundary layer instability, *J. Fluid Mech.* **12**, 1 (1961).
22. A. A. Szewczyk, Stability and transition of the free convection boundary layer along a flat plate, *Int. J. Heat Mass Transfer* **5**, 903 (1962).
23. P. Colak-Antic, Hitzdraht messungen des Laminar-Turbulenten Umschlags bei freier Konvektion, Jahrbuch der WGLR, p. 172 (1964).

24. Y. Jaluria and B. Gebhart, An experimental study of nonlinear disturbance behavior in natural convection, submitted for publication.
25. C. E. Polymeropoulos, A study of the stability of free convection flow over a uniform flux plate in nitrogen, PhD. Thesis, Cornell University (1966).
26. C. P. Knowles and B. Gebhart, An experimental investigation of laminar natural convection boundary layers, *Progress in Heat and Mass Transfer*, Vol 2, p. 99 (1969); See also: C. P. Knowles, A theoretical and experimental study of the stability of the laminar natural convection boundary layer over a vertical uniform flux plate, Ph.D. Thesis, Cornell University (1967).
27. E. Griffiths and A. H. Davis, The transmission of heat by radiation and convection, British food Investigation Board, Spec. Report 9, DSIR, London (1922).
28. O. A. Saunders, The effect of pressure upon natural convection in air, *Proc. R. Soc., Lond.* **157A**, 278 (1936).
29. O. A. Saunders, Natural convection in liquids, *Proc. R. Soc., Lond.* **172A**, 55 (1939).
30. E. R. G. Eckert and E. Soehngen, Interferometric studies on the stability and transition to turbulence of a free convection boundary layer, Proc. Gen. Disc. Heat Transfer, London (1951).
31. E. R. G. Eckert, J. P. Harnett and T. F. Irvine, Jr., Flow visualization studies of transition in turbulence in free convection, ASME paper No. 60-WA-250 (1960).
32. J. Coutanceau, Convection naturelle turbulente sur une plaque verticale isotherme, échange de chaleur et frottement pariétal, lois de répartition de vitesse et de température, *Int. J. Heat Mass Transfer* **12**, 735 (1969).

ÉTUDE EXPERIMENTALE DE LA TRANSITION POUR LA CONVECTION NATURELLE LE LONG D'UNE SURFACE VERTICALE

Résumé—Les conditions de transition ont été mesurées dans l'eau en termes de température moyenne, de fluctuation de température, d'épaisseur de région thermique et de facteur de transition thermique. On a effectué aussi des mesures anémométriques. On a trouvé un mécanisme de transition "thermique" distinct. Cette transition commence en aval des premiers signes de la transition dynamique. Dans cette région de retard, la température moyenne et les perturbations prenent graduellement leur forme turbulente. De plus nos mesures indiquent que la transition n'est pas prévisible avec précision uniquement à partir du nombre de Grashof. Ces premiers résuitats indiquent que la quantité d'énergie thermique localement convectée est le meilleur critère de positionnement de la transition, aussi bien que des autres aspects moins saillants. Cette idée est confirmée par une analyse des résultats publiés antérieurement.

EXPERIMENTELLE STUDIE DES UMSCHLAGES DER NATÜRLICHEN KONVEKTIONSSTRÖMUNG NAHE EINER VERTIKALEN OBERFÄCHE

Zusammenfassung—An Wasser wurden Umschlagserscheinungen gemessen, mit den Parametern: mittlere und wechselnde Temperatur, thermische Schicht-Dicke und thermischer Umschlagsfaktor. Auch Anemometer -Messungen wurden durchgeführt. Ein örtlicher thermischer Umschlagsmechanismus wurde festgestellt. Er begann stromabwärts bei ersten Anzeichen des Umschlages des Geschwindigkeitsfeldes. In diesem Anlaufgebiet erreichen die mittlere Temperatur und die Störgrösse allmählich ihre turbulente Form. Ausserdem zeigen unsere Daten, dass Umschlagserscheinungen allein in Abhängigkeit von der lokalen Grashof-Zahl nicht exakt bestimmbar sind. Diese ersten Ergebnisse lassen erkennen, dass die örtliche Grösse der konvektiven Wärmemenge eine viel bessere Einflussgrösse zur örtlichen Bestimmung des Umschlages darstellt als andere weniger ausgeprägte Eigenschaften des Umschlages. Eine Nachprüfung bereits veröffentlicher Daten für den Umschlag stützen diese Erkenntnis.

ЭКСПЕРИМЕНТАЛЬНОЕ ИССЛЕДОВАНИЕ ПЕРЕХОДНОГО РЕЖИМА СВОБОДНОКОНВЕКТИВНОГО ТЕЧЕНИЯ У ВЕРТИКАЛЬНОЙ ПОВЕРКНОСТИ

Аннотация—Явления, возникающие в переходном режиме, исследовались в воде на основании измерений средней температуры и функтуаций температуры, толщины тепловой области и теплового коэффициента перехода. Производились также измерения с помощью анемометра. Выявлен четкий механизм «теплового» перехода, начинающегося ниже области, в которой проявляются первые признаки перехода скоростного поля. В этой области запаздывания величины средней температуры и возмущений постепенно принимают вид, характерный для турбулентного течения. Полученные данные указывают также на то, что явления перехода нельзя точно рассчитать только с помощью локального значения числа Грасгофа. Эти первые результаты свидетельствуют о том, что положение области перехода, а также другие менее заметные признаки переходного режима лучше всего определять по велиуине локальной тепловой энергии, расходуемой на конвекцию. Анализ ранее опубликованных данных по явлениям перехода подтверждает этот вывод.